

Bispecific T-cells Expressing Polyclonal Repertoire of Endogenous $\gamma\delta$ T-cell Receptors and Introduced CD19-specific Chimeric Antigen Receptor

Drew C Deniger^{1,2}, Kirsten Switzer¹, Tiejuan Mi¹, Sourindra Maiti¹, Lenka Hurton^{1,2}, Harjeet Singh¹, Helen Huls¹, Simon Olivares¹, Dean A Lee^{1,2}, Richard E Champlin³ and Laurence JN Cooper^{1,2}

¹Division of Pediatrics, Children's Cancer Hospital, The University of Texas MD Anderson Cancer Center, Houston, Texas, USA; ²The University of Texas Graduate School of Biomedical Sciences at Houston, Houston, Texas, USA; ³Stem Cell Transplantation and Cellular Therapy, The University of Texas MD Anderson Cancer Center, Houston, Texas, USA

Even though other $\gamma\delta$ T-cell subsets exhibit antitumor activity, adoptive transfer of $\gamma\delta$ T cells is currently limited to one subset (expressing V γ 9V δ 2 T-cell receptor (TCR)) due to dependence on aminobisphosphonates as the only clinically appealing reagent for propagating $\gamma\delta$ T cells. Therefore, we developed an approach to propagate polyclonal $\gamma\delta$ T cells and rendered them bispecific through expression of a CD19-specific chimeric antigen receptor (CAR). Peripheral blood mononuclear cells (PBMC) were electroporated with *Sleeping Beauty* (SB) transposon and transposase to enforce expression of CAR in multiple $\gamma\delta$ T-cell subsets. CAR⁺ $\gamma\delta$ T cells were expanded on CD19⁺ artificial antigen-presenting cells (aAPC), which resulted in >10⁹ CAR⁺ $\gamma\delta$ T cells from <10⁶ total cells. Digital multiplex assay detected TCR mRNA coding for V δ 1, V δ 2, and V δ 3 with V γ 2, V γ 7, V γ 8, V γ 9, and V γ 10 alleles. Polyclonal CAR⁺ $\gamma\delta$ T cells were functional when TCR $\gamma\delta$ and CAR were stimulated and displayed enhanced killing of CD19⁺ tumor cell lines compared with CAR^{neg} $\gamma\delta$ T cells. CD19⁺ leukemia xenografts in mice were reduced with CAR⁺ $\gamma\delta$ T cells compared with control mice. Since CAR, SB, and aAPC have been adapted for human application, clinical trials can now focus on the therapeutic potential of polyclonal $\gamma\delta$ T cells.

Received 23 August 2012; accepted 28 November 2012; advance online publication 8 January 2013. doi:10.1038/mt.2012.267

INTRODUCTION

Chimeric antigen receptors (CARs) re-direct T-cell specificity to tumor-associated antigens (TAAs), such as CD19, independent of major histocompatibility complex.^{1–5} This genetic modification of T cells has clinical applications as adoptive transfer of CAR⁺ T cells with specificity for CD19 can lead to antitumor responses in patients with refractory B-cell malignancies.^{6–9} Current trials administer CAR⁺ T cells coexpressing $\alpha\beta$ T-cell receptor (TCR $\alpha\beta$) derived from a population that represents 95% of the peripheral T-cell pool. However, the remaining 1–5% of circulating T cells expressing TCR $\gamma\delta$ ($\gamma\delta$ T cells) have clinical appeal based on their

endogenous cytotoxicity toward tumor cells as well as their ability to present TAA and elicit an antitumor response.^{10–12} This population of T cells directly recognizes TAA, e.g., heat shock proteins, major histocompatibility complex class I chain-related gene A/B, F1-ATPase, and intermediates in cholesterol metabolism (phosphoantigens), in humans.¹³ Therefore, broad recognition of tumor cells and antitumor activity is achieved by these T cells expressing a diverse TCR $\gamma\delta$ repertoire (combination of V δ 1, V δ 2, or V δ 3 with one of fourteen V γ chains).¹⁴

T cells expressing V δ 1 and V δ 2 have been associated with anti-tumor immunity, but current adoptive immunotherapy approaches are limited to the V δ 2 subpopulation due to limited expansion methods of V δ 1 to clinically sufficient numbers of cells for human applications. For the most part, $\gamma\delta$ T cells have been numerically expanded *in vivo* and *ex vivo* using Zoledronic acid (Zol),¹⁵ an aminobisphosphonate that results in selective proliferation of T cells expressing V γ 9V δ 2 TCR.^{10,12,16} This treatment modality has resulted in objective clinical responses against both solid and hematologic tumors, but has not been curative as a monotherapy. V δ 1 $\gamma\delta$ T cells have not yet been infused, but their presence has correlated with complete responses observed in patients with B-cell acute lymphoblastic leukemia after undergoing $\alpha\beta$ T cell-depleted allogeneic hematopoietic stem cell transplantation.^{17–20} As both of these subpopulations of $\gamma\delta$ T cells are associated with antitumor activity, but have not been combined for cell therapy, we sought a clinically appealing approach to propagate T cells that maintain a polyclonal TCR $\gamma\delta$ repertoire.

Recognizing that a CD19-specific CAR can sustain the proliferation of $\alpha\beta$ T cells on artificial antigen-presenting cells (aAPC) independent of TCR $\alpha\beta$ usage,²¹ we hypothesized that $\gamma\delta$ T cells would expand on aAPC independent of TCR $\gamma\delta$. Our approach was further stimulated by the observation that K562, the cell line from which the aAPC were derived, is a natural target for $\gamma\delta$ T cells.¹⁸ We report that CAR⁺ $\gamma\delta$ T cells can be propagated to clinically relevant numbers on designer aAPC while maintaining a polyclonal population of TCR $\gamma\delta$ as assessed by our “direct TCR expression assay” (DTEA), a novel digital multiplexed gene expression analysis that we adapted to interrogate all TCR $\gamma\delta$ isotypes.²² These CAR⁺ $\gamma\delta$ T cells displayed enhanced killing of CD19⁺ tumor cell

Correspondence: Laurence JN Cooper, UT MD Anderson Cancer Center, Pediatrics, Unit 907, 1515 Holcombe Blvd., Houston, Texas 77030, USA. E-mail: ljncooper@mdanderson.org

lines *in vitro* compared with polyclonal $\gamma\delta$ T cells not expressing CAR. Leukemia xenografts in immunocompromised mice were significantly reduced when treated with CAR⁺ $\gamma\delta$ T cells compared with control mice. This study highlights the ability of aAPC to numerically expand bispecific T cells that exhibit introduced specificity for CD19 and retain endogenous polyclonal TCR $\gamma\delta$ repertoire.

RESULTS

CAR⁺ $\gamma\delta$ T cells numerically expand on aAPC

To date, it has been problematic to synchronously manipulate and expand multiple $\gamma\delta$ T-cell subpopulations for application in humans. Viral-mediated gene transfer typically requires cell division to achieve stable gene transfer and CARs have been introduced into transduced T cells expressing just V δ 2 TCR following the use of aminobisphosphonates to drive proliferation.²³ In contrast, non-viral gene transfer with *Sleeping Beauty* (SB) transposition can be achieved in quiescent peripheral blood mononuclear cells (PBMC) with the full complement of peripheral $\gamma\delta$ T cells initially present. Thus, stable expression of CAR can be achieved without prior T-cell propagation, enabling us to investigate whether a population of T

cells expressing polyclonal TCR $\gamma\delta$ chains could then be numerically expanded in a CAR-dependent manner on designer aAPC. PBMC were electroporated (day 0) with SB transposon/transposase system to enforce expression of a second generation CD19-specific CAR (CD19RCD28)⁵ that signals through chimeric CD28 and CD3- ζ . Electroporated cells were sorted using paramagnetic beads to separate the $4.0 \pm 1.5\%$ (mean \pm SD; $n = 4$) CAR⁺ $\gamma\delta$ T cells from the majority of CAR⁺ $\alpha\beta$ T cells. The CAR⁺ $\gamma\delta$ T cells were selectively propagated by the recursive additions of γ -irradiated K562-derived aAPC (clone #4, genetically modified to coexpress CD19, CD64, CD86, CD137L, and membrane bound interleukin (IL)-15)⁵ with soluble IL-2 and IL-21. IL-21 is included in the manufacture of our CAR⁺ $\alpha\beta$ T cells so it was used to propagate CAR⁺ $\gamma\delta$ T cells.⁵ Prior experiments predicted that IL-2 and IL-15 enhance the proliferative potential of $\gamma\delta$ T cells, and synergy between IL-2 and IL-21 has led to improved antitumor activity compared with $\gamma\delta$ T cells grown with either IL-2 or IL-21 alone.^{24–28} Sham electroporations were undertaken to provide staining control T cells that were propagated by cross-linking CD3 using aAPC loaded with OKT3 to numerically expand CAR^{neg} $\alpha\beta$ T cells.²⁹ As expected, CAR was expressed on the day following electroporation (day 1) in most of

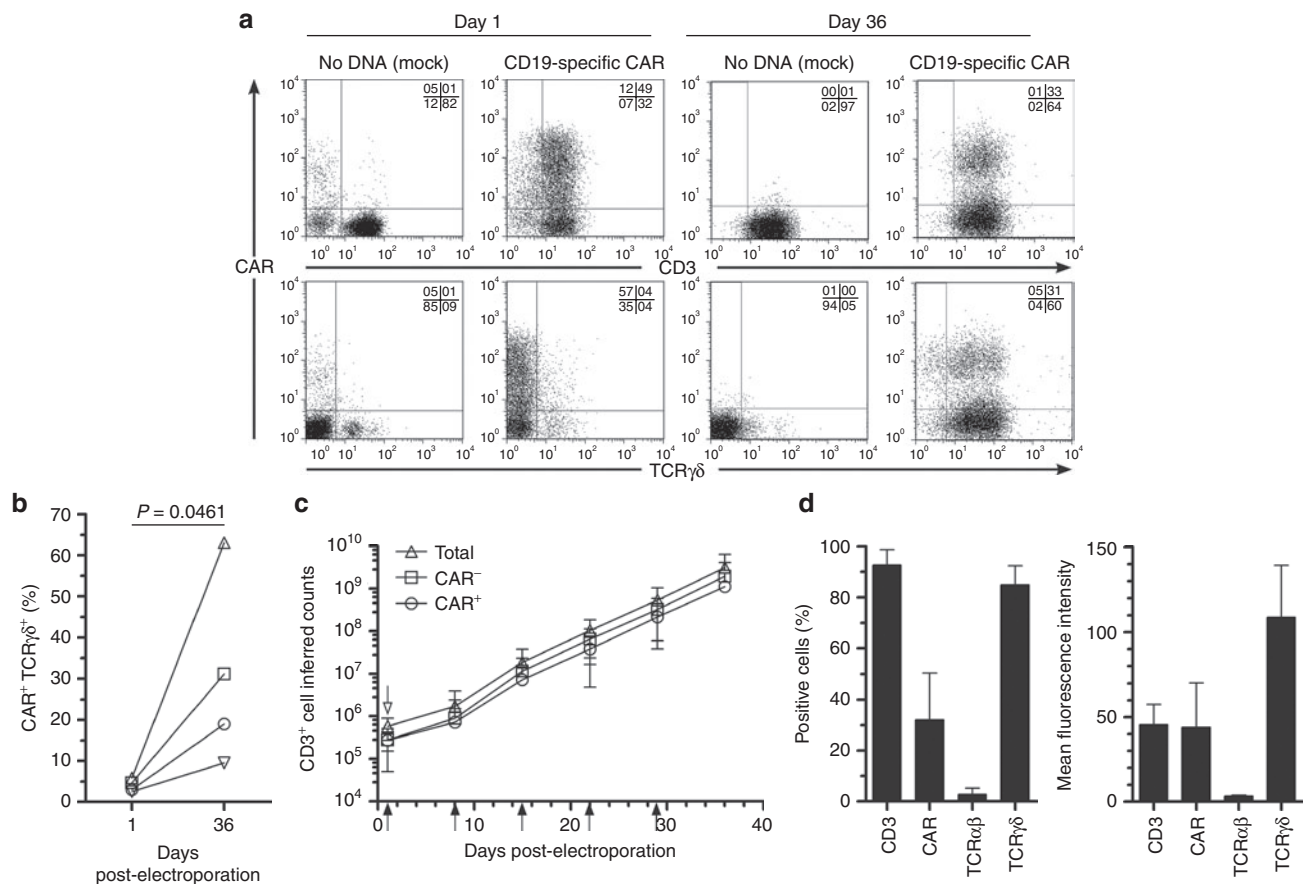


Figure 1 CAR⁺ $\gamma\delta$ T cells propagate on designer aAPC. **(a)** Transient (day 1) and stable (day 36) expression of CAR in T cells (top) and $\gamma\delta$ T cells (bottom) in mock electroporated ("no DNA") or CD19-specific CAR-electroporated cells (CD19RCD28). **(b)** Percentage of CAR⁺ $\gamma\delta$ T cells in the culture as transient (day 1) and stable (day 36) expression, where each shape represents an individual donor. **(c)** Rate of expansion of total $\gamma\delta$ T cells (open triangles), CAR^{neg} $\gamma\delta$ T cells (open squares), and CAR⁺ $\gamma\delta$ T cells (open circles) over tissue culture period following paramagnetic bead sorting (open arrow) and recursive stimulation (closed arrows) with aAPC and exogenous IL-2 and IL-21 administration. **(d)** Percentage-positive cells and mean fluorescence intensity of CD3, CAR, TCR $\alpha\beta$, and TCR $\gamma\delta$ at day 36. Data are mean \pm SD ($n = 4$) and quadrant percentages of flow plots are in upper right corner. aAPC, artificial antigen-presenting cell; *** $P < 0.001$. CAR, chimeric antigen receptor; IL, interleukin; TCR, T-cell receptor.

the T cells, including $\gamma\delta$ T cells, which comprised up to 10% of the mononuclear cells (Figure 1a, left). After 36 days of co-culture on aAPC, the majority of cells coexpressed CD3 and TCR $\gamma\delta$ with $30.7 \pm 23.3\%$ ($n = 4$) CAR expression (Figure 1a, right). The absolute CAR proportions at day 36 varied in frequency depending on the donor, but increased compared with the initial populations of CAR $^+$ $\gamma\delta$ T cells at day 1 (Figure 1b). As we have demonstrated, our aAPC co-culture system enforces CAR expression in $\alpha\beta$ T cells (>90% CAR $^+$ T cells by 28 days of co-culture),⁵ but the apparent lack of the same degree of selective pressure when combined with $\gamma\delta$ T cells was attributed to an inherent ability of CAR $^{\text{neg}}\gamma\delta$ T cells to sustain proliferation on aAPC derived from K562. Continuous proliferation of both CAR $^{\text{neg}}$ and CAR $^+$ $\gamma\delta$ T cells was observed over the tissue culture period. Even so, we could generate up to $1.5 \times 10^9 \pm 1.2 \times 10^9$ ($n = 3$) CAR $^+$ $\gamma\delta$ T cells from the $2.8 \times 10^5 \pm 1.5 \times 10^5$ ($n = 3$) CAR $^+$ $\gamma\delta$ T cells at the start of the culture (Figure 1c). Most of the propagated cells coexpressed CD3 and TCR $\gamma\delta$, but did not express TCR $\alpha\beta$ (Figure 1d). These data demonstrate that aAPC could be used to sustain proliferation of CAR $^+$ T cells coexpressing TCR $\gamma\delta$.

Immunophenotype of numerically expanded CAR $^+$ $\gamma\delta$ T cells

Multiparameter flow cytometry was used to gate on CAR $^+$ T cells and analyze their expression of cell surface markers (Figure 2). TCR $\gamma\delta$ was expressed at high and low densities (Figure 2a, top). CD56, a marker of major histocompatibility complex-unrestricted lytic ability,³⁰ was also expressed on T cells, but the culture contained <1% CD3 $^{\text{neg}}$ CD56 $^+$ natural killer cells and <1% CD3 $^+$ V α_{25} TCR $^+$ NK T cells (data not shown). In contrast to $\alpha\beta$ T cells, no CAR $^+$ $\gamma\delta$ T cells expressed CD4, some were CD8 $^+$, but most were CD4 $^{\text{neg}}$ CD8 $^{\text{neg}}$, which is consistent with what is known for $\gamma\delta$ T cells.³¹ The relative frequencies for each donor are shown in Figure 2b. Markers associated with memory, e.g., CD27, CD28, CD62L, and CCR7, were expressed by CAR $^+$ $\gamma\delta$ T cells (Figure 2a, bottom). Both naive (CD45RA) and antigen-experienced (CD45RO) cells were present after

propagation on aAPC, and the T cells were not exhausted as measured by low expression of CD57 (Figure 2b). In aggregate, cultures contained a heterogenous mixture of naive (CD45RA $^+$ CD27 $^+$ CD28 $^+$ CCR7 $^+$; $26.5 \pm 6.2\%$), central memory (CD45RA $^{\text{neg}}$ CD27 $^+$ CD28 $^+$ CCR7 $^+$; $7.8 \pm 3.6\%$), effector memory (CD45RA $^{\text{neg}}$ CD27 $^+$ CD28 $^{\text{neg}}$ CCR7 $^{\text{neg}}$; $10.1 \pm 5.4\%$), and effector memory RA (CD45RA $^+$ CD27 $^{\text{neg}}$ CD28 $^{\text{neg}}$ CCR7 $^{\text{neg}}$; $7.6 \pm 3.4\%$) T-cell phenotypes.^{32,33} Costimulation by enforced expression of CD86 and CD137L (4-1BBL) on aAPC may be important for CAR $^+$ $\gamma\delta$ T-cell numeric expansion due to expression of their receptors CD28 and CD137 (4-1BB), respectively. Molecules associated with homing to bone marrow (cutaneous lymphocyte antigen and CXCR4) and lymph nodes (CD62L and CCR7) were present on CAR $^+$ $\gamma\delta$ T cells suggesting that they could migrate to sites known to harbor leukemia. In sum, propagated CAR $^+$ $\gamma\delta$ T cells expressed T cell-associated surface markers that indicate desired potential for memory and homing.

Direct TCR expression assay to reveal γ and δ TCR usage in CAR $^+$ $\gamma\delta$ T cells

We sought to determine that aAPC-propagated CAR $^+$ T cells were indeed bispecific as defined by the presence of a polyclonal population of TCR $\gamma\delta$ alleles. Up to now, it has been difficult to determine the pattern of expression of the γ and δ TCR chains. Therefore, we adapted our DTEA to assess the complete TCR $\gamma\delta$ transcriptome. This approach takes advantage of the nCounter assay system to measure multiple bar-coded genes in a single reaction with high sensitivity and linearity across a broad range of expression.³⁴ A multiplexed CodeSet was designed with two sequence-specific probes for each allele to evaluate TCR $\gamma\delta$ isotypes. The DTEA was initially validated using Zol to preferentially propagate V γ 9V δ 2 cells from PBMC and, as expected, the resultant TCR usage was dominated by both V δ 2 and V γ 9 at protein and mRNA levels (Supplementary Figure S1). A second validation employed antibodies directed against $\gamma\delta$ T-cell subsets (V δ 1 and V δ 2) to measure their mRNA expression. V δ 1 $^{\text{neg}}$ V δ 2 $^{\text{neg}}$, V δ 1 $^+$ V δ 2 $^{\text{neg}}$, and V δ 1 $^{\text{neg}}$ V δ 2 $^+$ cells were sorted from CAR $^{\text{neg}}$ T cells (to maximize

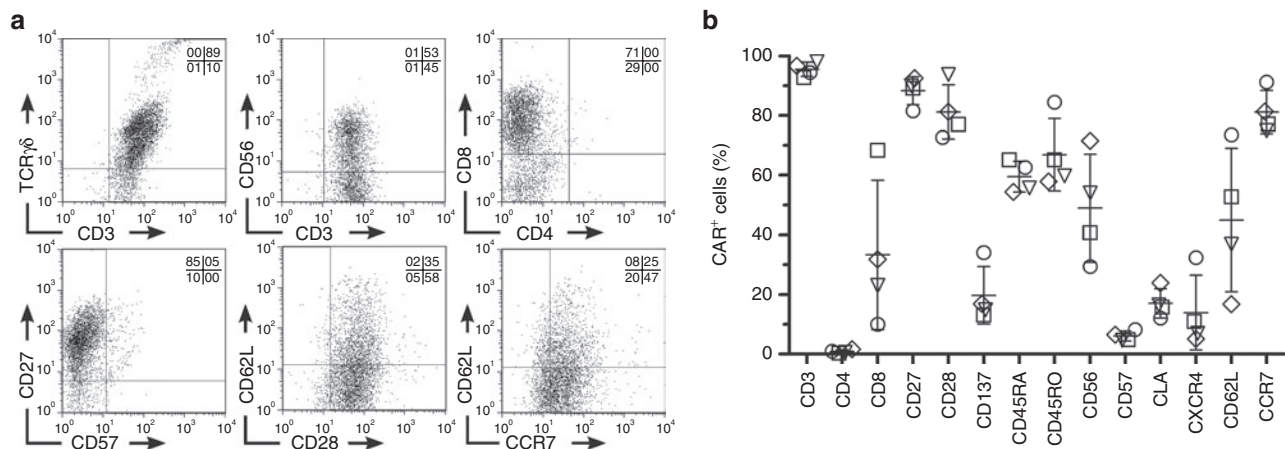


Figure 2 Immunophenotype of electroporated, separated, and propagated CAR $^+$ $\gamma\delta$ T cells. **(a)** Expression by flow cytometry of cell surface markers associated with T cells and memory as gated on CD3 $^+$ CAR $^+$ cells. **(b)** Percentages of CAR $^+$ T cells expressing T-cell markers, where each shape represents a different donor. Data are mean \pm SD ($n = 4$). Quadrant percentages of flow plots are in upper right corner. CAR, chimeric antigen receptor; TCR, T-cell receptor.

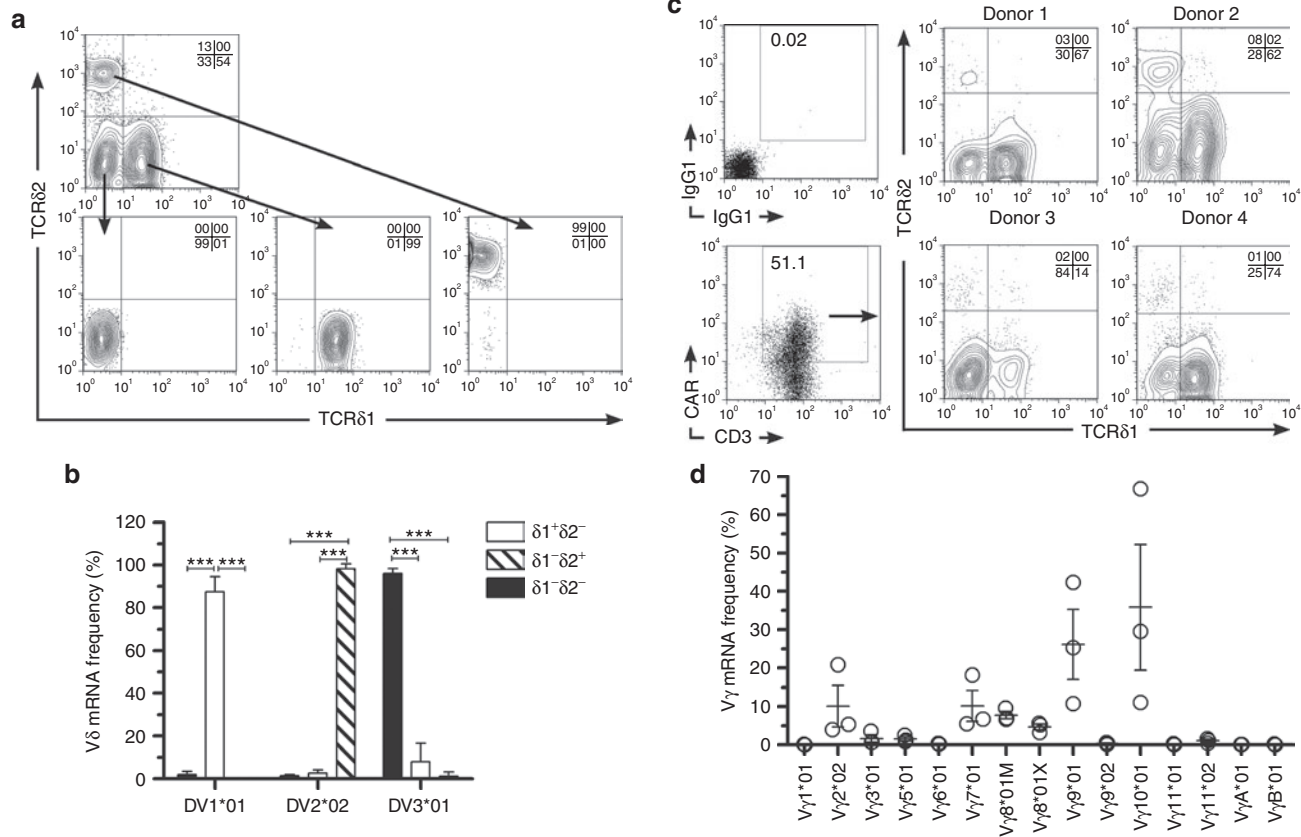


Figure 3 Distribution of $V\delta$ and $V\gamma$ in $CAR^+\gamma\delta$ T cells. **(a)** Representative FACS of $V\delta$ populations (top) into $V\delta1^{neg}V\delta2^{neg}$ (left), $V\delta1^+V\delta2^{neg}$ (middle), and $V\delta1^{neg}V\delta2^+$ (right) populations and **(b)** $V\delta$ allele mRNA expression in sorted T cells. **(c)** $V\delta1^{neg}V\delta2^{neg}$, $V\delta1^+V\delta2^{neg}$, and $V\delta1^{neg}V\delta2^+$ frequencies in gated $CAR^+\gamma\delta$ T-cell populations from four donors. **(d)** $V\gamma$ allele mRNA expression in $CAR^+\gamma\delta$ T cells. Data are mean \pm SD ($n = 3$). Quadrant percentages of flow plots are in upper right corner. *** $P < 0.001$. CAR, chimeric antigen receptor; FACS, fluorescence-activated cell sorting; TCR, T-cell receptor.

the number of $V\delta2$ cells recovered by fluorescence-activated cell sorting (FACS) and subjected to DTEA (Figure 3a). As expected, $V\delta1^+V\delta2^{neg}$, $V\delta1^{neg}V\delta2^+$, and $V\delta1^{neg}V\delta2^{neg}$ expressed $V\delta1*01$, $V\delta2*02$, and $V\delta3*01$ mRNA species, respectively (Figure 3b). These two strategies supported the validity of the DTEA panel enabling the identity of $TCR\gamma\delta$ to be determined in CAR^+ T cells. Therefore, we measured the mRNA levels for all three $V\delta$ alleles as present in electroporated, separated, and propagated $CAR^+\gamma\delta$ T cells which correlated with multiparameter flow cytometry on gated CAR^+ T cells to reveal the frequencies of $V\delta$ subsets based on protein expression. The three $V\delta$ populations were present in ascending frequency ($V\delta1 > V\delta3 >> V\delta2$) in the electroporated and propagated T cells (Figure 3c). $CAR^{neg}\gamma\delta$ T cells displayed similar frequencies of $V\delta$ TCR usage as $CAR^+\gamma\delta$ T cells. DTEA array also assessed $V\gamma$ usage, which is of particular utility because only one antibody against $V\gamma9$ is commercially available, thus limiting the tools with which to detect $V\gamma$ usage. Of note, $V\gamma2$, $V\gamma7$, $V\gamma8$ (both alleles), $V\gamma9$, and $V\gamma10$ were present in CAR^+ T-cell cultures (Figure 3d). A lack of commercially available antibodies prevented assessment of pairing between individual $V\delta$ and $V\gamma$ chains on the T cells. The TCR usage described for $\gamma\delta$ T cells was that which was present at the time of functional assays. Our ability to digitally quantify the presence of mRNA species enabled us to determine that the propagated CAR^+ T cells expressed a polyclonal population of $TCR\gamma\delta$ chains.

T cells produced proinflammatory cytokines in response to stimulation through endogenous $TCR\gamma\delta$ and introduced CAR

The functional activity of the CAR^+ T cells was assessed by activation with leukocyte activation cocktail, which was comprised of phorbol 12-myristate 13-acetate and ionomycin. Leukocyte activation cocktail mimics activation through TCR by simulating protein kinase C and increasing intracellular Ca^{2+} to activate phospholipase C. Measurement of secreted and intracellular cytokines (in the presence of the inhibitor GolgiPlug, which contains brefeldin A) were performed on genetically modified T cells with and without leukocyte activation cocktail (Figure 4a,b). A broad range of cytokines were produced by $\gamma\delta$ T cells, with the highest expression of interferon- γ (IFN γ), tumor necrosis factor- α , and chemokines macrophage inflammatory protein (MIP)-1 α , MIP-1 β , and regulated and normal T cell expressed and secreted (Figure 4b). IL-17 has been shown to be important for antitumor efficacy of $\gamma\delta$ T cells and this cytokine was secreted by $CAR^+\gamma\delta$ T cells. These results suggest that $TCR\gamma\delta$ can be activated to produce cytokines that could promote inflammation within the tumor. Next, CAR-specific cytokine production was assessed by activation using the murine T-cell lymphoma line EL4 and a genetically modified derivative to enforce expression of human CD19. Both tumor necrosis factor- α and IFN γ were produced by $CAR^+\gamma\delta$ T cells in response to CD19 (Figure 4c). A less diverse repertoire of cytokines was secreted

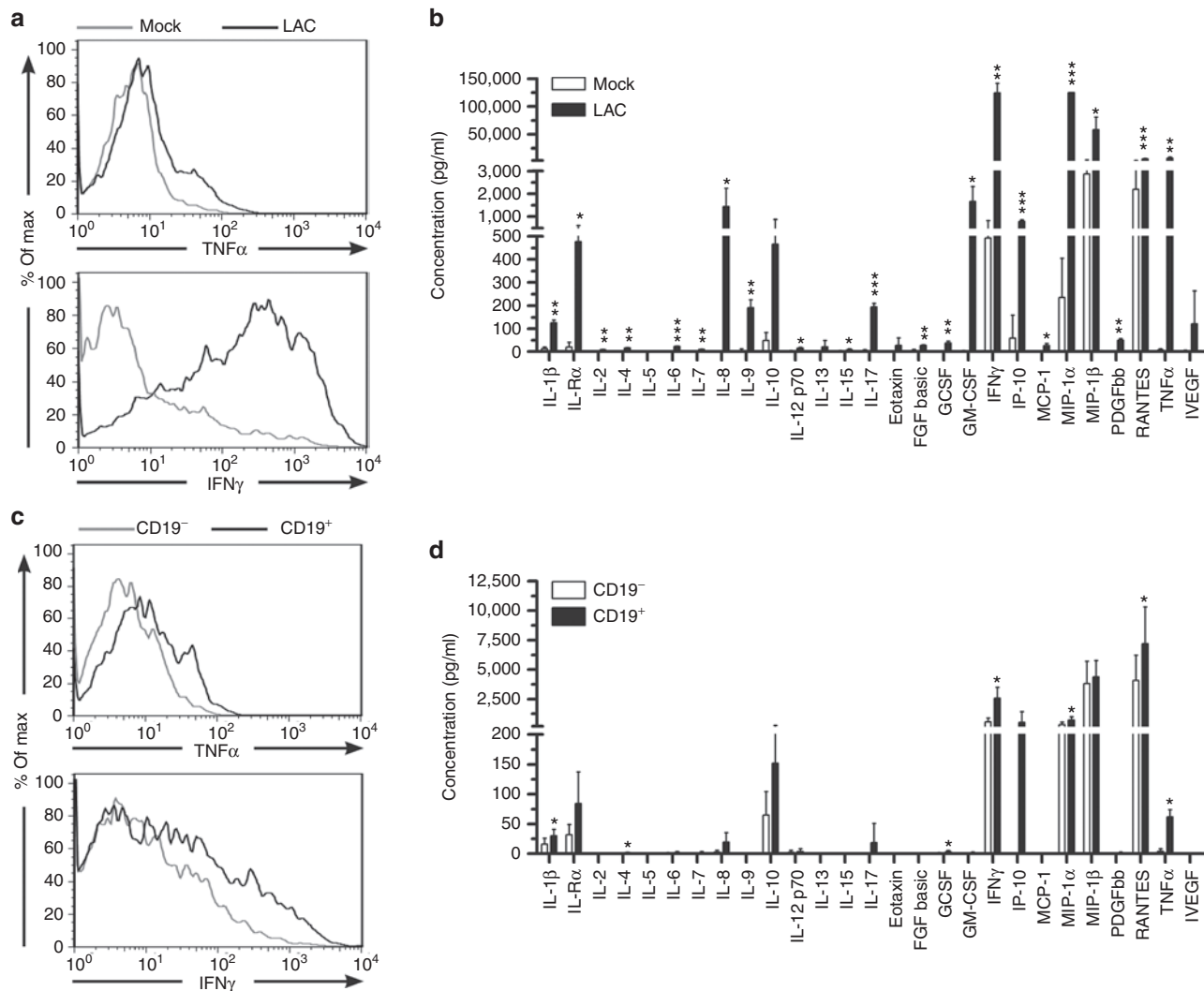


Figure 4 Bispecific $\gamma\delta$ T cells produce proinflammatory cytokines when endogenous TCR and introduced CAR are stimulated. **(a)** CAR⁺ $\gamma\delta$ T cells at day 35 of co-culture on aAPC were stimulated for 4 hours with a mock cocktail (media alone) or leukocyte activation cocktail (LAC, PMA/ionomycin) to induce TCR stimulation and then analyzed by flow cytometry. CAR⁺ T cells were gated and tumor necrosis factor- α (TNF- α , top) and interferon- γ (IFN- γ , bottom) production is shown. **(b)** Luminex array (27-Plex) of cytokines secreted by CAR⁺ $\gamma\delta$ T cells in conditions described in **a**. **(c)** Similar to **a** except that EL4-CD19^{neg} and EL4-CD19⁺ were used instead of mock/LAC. **(d)** Same as **b** but with EL4-CD19^{neg} and EL4-CD19⁺ targets. Student's *t*-test for statistical analysis between mock and LAC (in **b**) and EL4-CD19^{neg} and EL4-CD19⁺ (in **d**) where **P* < 0.05, ***P* < 0.01, and ****P* < 0.001. Data are representative of four donors for **a** and **c** and mean \pm SD (*n* = 3) for **b** and **d**. aAPC, artificial antigen-presenting cell; CAR, chimeric antigen receptor; FGF, fibroblast growth factor; GM-CSF, granulocyte-macrophage colony-stimulating factor; IL, interleukin; MCP, monocyte chemoattractant protein; MIP, macrophage inflammatory protein; PDGFbb, platelet-derived growth factor- β ; PMA, phorbol 12-myristate 13-acetate; RANTES, regulated and normal T cell expressed and secreted; TCR, T-cell receptor; VEGF, vascular endothelial growth factor.

following CAR stimulation when compared with stimulation of TCR $\gamma\delta$, but IFN γ , tumor necrosis factor- α , MIP-1 α , MIP-1 β , and regulated and normal T cell expressed and secreted were all increased in response to activation through CAR (Figure 4d). In aggregate, proinflammatory cytokines were upregulated by bispecific CAR⁺ $\gamma\delta$ T cells through their TCR and CAR.

CAR⁺ $\gamma\delta$ T cells exhibit enhanced antitumor effects against CD19⁺ targets *in vitro*

It was anticipated that $\gamma\delta$ T cells would display endogenous cytotoxicity to leukemia cells. Therefore, $\gamma\delta$ T cells without CAR were numerically expanded on aAPC in order to test their antileukemia activity. Human CD19⁺ B-cell acute lymphoblastic leukemia cell

lines (REH, Kasumi-2, and Daudi genetically modified to express β 2M) were lysed by CAR^{neg} $\gamma\delta$ T cells while primary, healthy CD19⁺ B cells were not killed by the same effectors (Figure 5a). However, not all B-cell acute lymphoblastic leukemia cell lines were susceptible to efficient lysis by CAR^{neg} $\gamma\delta$ T cells. In particular, EL4 and NALM-6 cells were largely resistant to cytotoxicity by $\gamma\delta$ T cells. Thus, the ability of the CD19-specific CAR to amplify the inherent antitumor activity of $\gamma\delta$ T cells was investigated. Enforced expression of CD19 on the surface of EL4 cells improved targeting and killing of this cell line by CAR⁺ $\gamma\delta$ T cells at significantly higher (*P* = 0.0001) levels compared with the parental CD19^{neg} EL4 cell line (Figure 5b). Similarly, CAR⁺ $\gamma\delta$ T cells exhibited improved ability (*P* = 0.001) to kill CD19⁺ NALM-6 cells compared with CAR^{neg} $\gamma\delta$

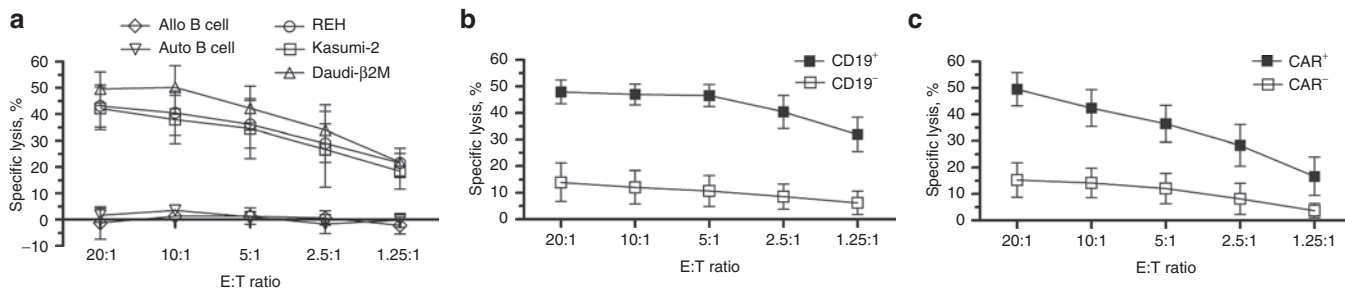


Figure 5 Specific lysis of CD19⁺ tumor cell lines by CAR⁺ $\gamma\delta$ T cells. (a) Standard 4-hour CRA of (a) CAR^{neg} $\gamma\delta$ T cells against CD19⁺ B-ALL cell lines (REH, Kasumi-2, and Daudi- β 2M) or primary CD19⁺ B cells from autologous (Auto) or allogeneic (Allo) donors, (b) CAR⁺ $\gamma\delta$ T cells against EL4-CD19^{neg} (open squares) and EL4-CD19⁺ (closed squares) tumor cells, and (c) CAR^{neg} $\gamma\delta$ T cells (open squares) and CAR⁺ $\gamma\delta$ T cells (closed squares) against CD19⁺ NALM-6 tumor cells. Data are mean \pm SD from four healthy donors (average of triplicate measurements for each donor) that were pooled from two independent experiments. B-ALL, B-cell acute lymphoblastic leukemia; CAR, chimeric antigen receptor; CRA, chromium release assay; E:T, effector to target ratio.

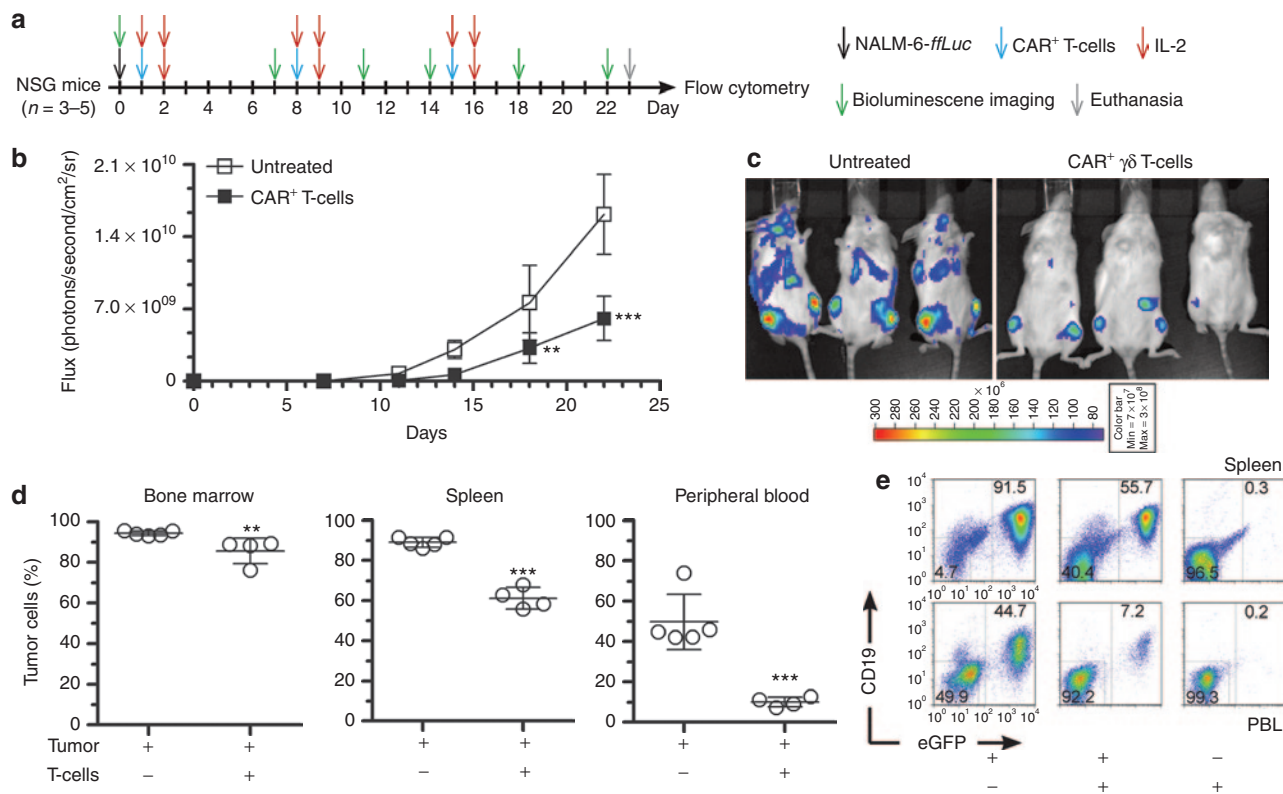


Figure 6 *In vivo* antitumor activity of CAR⁺ $\gamma\delta$ T cells. (a) Schematic of experiment. (b) BLI derived from eGFP⁺*ffLuc*⁺CD19⁺ NALM-6 tumor and (c) representative images of mice at day 22. (d) Postmortem analysis of tissues and blood where tumor cells (CD19⁺eGFP⁺) were detected by flow cytometry. (e) Representative flow plots from d. Data are mean \pm SD ($n = 3-5$ mice per group, representative of two independent experiments) and gating frequencies in e are displayed. The percentage of tumor cells is derived from detecting CD19⁺eGFP⁺NALM-6 by flow cytometry from postmortem samples. Statistics performed with (in b) two-way ANOVA with Bonferroni's post-tests and (in d) Student's *t*-test between treated and untreated mice. ** $P < 0.01$ and *** $P < 0.001$. ANOVA, analysis of variance; BLI, bioluminescent imaging; CAR, chimeric antigen receptor; eGFP, enhanced green fluorescent protein; IL, interleukin; PBL, peripheral blood leukocyte.

T cells (Figure 5c). In summary, the introduced CAR enhanced the specific killing capability of genetically modified $\gamma\delta$ T cells.

CAR⁺ $\gamma\delta$ T cells can target CD19⁺ tumor *in vivo*

The ability of electroporated and propagated $\gamma\delta$ T cells to target CD19⁺ tumor was then investigated *in vivo*. NALM-6 is an aggressive CD19⁺ B-cell leukemia model and immunocompromised mice engrafted with 10⁵ NALM-6 are moribund in 20–25

days when untreated. Control of disseminated NALM-6 tumor *in vivo* is dependent on the infused T cells homing to tumor and activating cytolytic machinery in the tumor microenvironment. After adoptive immunotherapy, the burden of tumor was significantly decreased in mice receiving CAR⁺ $\gamma\delta$ T cells (donor no. 4 from Figure 3c) compared with untreated mice (Figure 6). Mice in treatment group receiving CAR⁺ T cells displayed fewer characteristics of the untreated and thus unwell mice, which included

lethargy, ruffled coat, temporary hind limb paralysis, and difficulty entering and exiting anesthesia at late stages of the experiment. A uniform date for euthanasia was chosen to measure the anti-tumor effect based on flow cytometry for NALM-6 in lymphoid tissue. There was significant antitumor activity by the CAR⁺ $\gamma\delta$ T cell as measured by bioluminescent imaging of NALM-6-eGFP-*ffLuc* (Figure 6b) as exemplified at 22 days after injection of tumor (Figure 6c). Noninvasive imaging was corroborated by analysis of presence of tumor cells at necropsy. Mice that received CAR⁺ $\gamma\delta$ T cells exhibited significant reductions in tumor burden (CD19⁺eGFP⁺) in the bone marrow, spleen, and peripheral blood (Figure 6d,e). These data reveal that polyclonal CAR⁺ $\gamma\delta$ T cells exhibit therapeutic activity *in vivo*.

DISCUSSION

We established that introduction of a second generation CAR could (i) drive the numeric expansion of T cells independent of usage of TCR $\gamma\delta$ chains and (ii) augment the lytic potential of CD19⁺ tumors by $\gamma\delta$ T cells. Propagating bispecific CAR⁺ T cells with a broad diversity of TCR $\gamma\delta$ chains are desirable based on their therapeutic potential. Indeed, $\gamma\delta$ T cells other than those expressing V γ 9V δ 2 have been generated from PBMC using TCR $\gamma\delta$ -specific and CD3-specific monoclonal antibodies.³⁵⁻³⁷ These prior approaches did not comprehensively measure TCR $\gamma\delta$ isotype expression nor did they yield V δ 1 and V δ 3 at frequencies as high as seen in this study. The V γ 2 TCR chain was detected on our T cells, which has been described to pair with V δ 2, and these T cells can have antigen presentation capabilities.³⁸ Our CAR⁺ $\gamma\delta$ T cells expressed molecules consistent with antigen presentation, e.g., CD86, CD137L, and human leukocyte antigen-DR (data not shown), and V γ 9V δ 2 cells have served as aAPC for $\alpha\beta$ T cells.¹¹ Future experiments will investigate whether our polyclonal CAR⁺ $\gamma\delta$ T cells also have an ability to serve as aAPC. Also present were T-cell subpopulations expressing V γ 7, V γ 8, and V γ 10, where the first two chains have been associated with intestinal intraepithelial lymphocytes^{39,40} and the latter chain's functional significance is not yet apparent. In all, our approach is the first to report expansion of CAR⁺ T cells that maintained a polyclonal TCR $\gamma\delta$ expression.

The repertoire of TCR $\gamma\delta$ chains employed by CAR⁺ T cells was similar to the initial pool of $\gamma\delta$ T cells in PBMC with two exceptions. We noted an increase in V δ 3 usage, but this may be advantageous as it is associated with specificity for viruses that could offer enhanced immune responses to viral infections in immunocompromised patients receiving therapy.⁴¹ A decrease in V γ 9V δ 2 usage was also observed compared with the starting frequency of this TCR in PBMC, but this could potentially be increased by priming aAPC with Zol to increase V γ 9V δ 2 ligand expression in the co-culture. Whether this loss of V γ 9V δ 2 TCR expression was due to preferential activation induced cell death or selective out-growth of T cells expressing V δ 1 and V δ 3TCR is not known. Nonetheless, V γ 9V δ 2 chains were still present in the final T-cell cultures indicating that aminobisphosphonate therapy could drive expansion of this subset of T cells after administration.

Recombinant retroviruses have been previously employed to achieve stable expression of CARs in $\gamma\delta$ T cells, but this required using an aminobisphosphonate to achieve numeric expansion of T cells before transduction.^{16,42} We now demonstrate propagation of

T cells after, rather than before, gene transfer using SB-mediated transposition results in a polyclonal population of bispecific $\gamma\delta$ T cells capable of CAR-mediated (i) production and secretion of pro-inflammatory cytokines in response to CD19, (ii) enhanced lysis of CD19⁺ tumor targets, and (iii) *in vivo* antitumor activity against a CD19⁺ tumor. The ability of these T cells to exhibit effector functions was not correlated to a particular V δ or V γ usage as cells with different V δ TCR frequencies (Figure 3c) produced the same cytokines (Figure 4) and displayed similar cytotoxicity of CD19⁺ targets (Figure 5b). We noted that frequency of CAR expression was more variable on $\gamma\delta$ T cells compared with $\alpha\beta$ T cells. This was likely due to an endogenous ability of K562 cells to sustain proliferation of $\gamma\delta$ T cells independent of CAR. Nevertheless, adoptive transfer of $\gamma\delta$ T cells of which 60% expressed CAR could still yield the same *in vitro* lytic ability as 98% CAR⁺ $\gamma\delta$ T cells (Supplementary Figure S2). This indicated that (i) CAR⁺ $\gamma\delta$ T cells are potent tumor killers and (ii) >90% CAR expression may not be a critically limiting parameter for predicting therapeutic efficacy. Nonetheless, we are undertaking improvements to increase the expression of CAR on propagated $\gamma\delta$ T cells. Furthermore, the chimeric signaling molecules in the CAR endodomain could be specifically designed to enhance triggering of $\gamma\delta$ T cells. For example, $\gamma\delta$ T cells can be activated through Fc γ RIIIA (CD16) in the TCR complex,⁴³ which raises the possibility that signaling through chimeric Fc γ (as compared with CD3- ζ in our current design) in a CAR endodomain may improve activation. However, CD16 was not detected on CAR⁺ $\gamma\delta$ T cells in this study (data not shown). Since clinical responses against CD19⁺ chronic lymphocytic leukemia have been achieved with T cells expressing a CAR that signaled through 4-1BB (CD137) endodomain,^{7,8} another option is to swap CD28 for CD137 for activation of $\gamma\delta$ T cells.

In addition to improving CAR expression on $\gamma\delta$ T cells, the type of $\gamma\delta$ T cell arising after electroporation with SB system and propagation on aAPC could be manipulated to further improve antitumor activity. For instance, some $\gamma\delta$ T cells were observed to secrete IL-17, a proinflammatory cytokine that has potent, yet context-dependent, antitumor effects.⁴⁴⁻⁴⁸ IL-17 producing lineages of T cells can be mutually exclusive from those that secrete IFN γ .⁴⁹ Inducible costimulator of T cells (ICOS) leads to IL-17 polarization in CD4⁺ T cells and CD28 costimulation overcame this effect to dictate that CD4⁺ T cells now produce IFN γ .⁵⁰ CD86 is one of the costimulatory molecules on our aAPC and the majority of CAR⁺ $\gamma\delta$ T cells secrete IFN γ in response to CD19 with diminished production of IL-17. Furthermore, the CAR contains a chimeric CD28 endodomain which may contribute to IFN γ polarization in genetically modified T cells. Substitution of chimeric CD28 for ICOS in the CAR and replacement of CD86 on the aAPC with ICOS-ligand could potentially reverse the polarization to IL-17. Given that we can propagate CAR⁺ $\gamma\delta$ T cells on aAPC, we are prepared to design aAPC to evaluate whether we can skew the cytokine profile to reflect the propagation of desired T-cell subsets.

The human application of CAR⁺ $\gamma\delta$ T cells is appealing given their inherent potential for antitumor effects and their apparent lack of alloreactivity.¹⁹ The CAR, SB system, and aAPC are all already in use in our clinical trials. Therefore, we plan to modify our manufacturing scheme in compliance with current good manufacturing practice to generate bispecific CAR⁺ $\gamma\delta$ T cells. Our data provides a

clinically appealing approach to numerically expand and manipulate CAR⁺ T cells with multiple V γ and V δ pairings enabling clinical trials to evaluate their therapeutic potential.

MATERIALS AND METHODS

Plasmids and cell lines. Codon-optimized DNA plasmids for SB transposase (SB11) and a second generation CD19-specific CAR (designated CD19RCD28) transposon are described elsewhere.⁵ NALM-6 and EL4 cell lines were acquired from Deutsche Sammlung von Mikroorganismen und Zellkulturen (DSMZ, Braunschweig, Germany) and American Type Culture Collection (Manassas, VA), respectively. Daudi expressing β 2 microglobulin and NALM-6 expressing firefly luciferase and enhanced green fluorescent protein (NALM-6-*ffLuc*-eGFP) were generated as previously described.⁵ Kasumi-2 and REH cell lines were provided by Dr Jeff Tyner (Oregon Health and Science University). A transposon (**Supplementary Figure S3**) containing neomycin phosphotransferase linked *via* F2A self-cleavable peptide sequences to human CD19 (truncated following its transmembrane domain) was used to express this TAA on EL4 cells following electroporation with SB11 transposase and Mouse T Cell Nucleofector Kit (cat. no. VPA-1006; Lonza, Basel, Switzerland) followed by subsequent selection under 0.8 mg/ml G418 (InvivoGen, San Diego, CA). K562-derived aAPC (clone #4) were used as previously described.^{5,51} Cell lines were maintained in complete media (RPMI, 10% heat-inactivated fetal bovine serum (Hyclone, Logan, UT), and 1% Glutamax-100 (Gibco, Grand Island, NY)), in humidified conditions with 5% CO₂ at 37°C. All cell line identities were confirmed by STR DNA Fingerprinting at the MDACC's Cancer Center Support Grant (CCGS) core facility.

T-cell propagation. PBMC were obtained after informed consent from healthy volunteers and isolated by Ficoll-Paque (GE Healthcare, Milwaukee, WI).¹ 10⁸ thawed PBMC were electroporated using program U-014 (on day 0 of co-culture) with 75 μ g supercoiled DNA plasmid coding for CD19RCD28 transposon and 25 μ g supercoiled DNA plasmid coding for SB11 transposase in cuvettes (2 \times 10⁷ cells per cuvette) using Nucleofector II and Human T cell Nucleofector Kit (Lonza).⁵ The following day (day 1), paramagnetic separation was performed with TCR γ/δ ⁺ T-cell isolation kit (cat. no. 130-092-892; Miltenyi Biotec, Auburn, CA) and LS columns (cat. no. 130-042-401; Miltenyi Biotec), which separated untouched $\gamma\delta$ T cells in the negative fraction from $\alpha\beta$ T cells attached to magnet. Also on day 1, CAR⁺ $\gamma\delta$ T cells were stimulated at a ratio of one CAR⁺ T cell to two γ -irradiated (100 Gy) aAPC (clone #4) in presence of exogenous IL-2 (50 U/ml, added three times per week; Novartis, Basel, Switzerland) and IL-21 (30 ng/ml, added three times per week; eBioscience, San Diego, CA). Cells were serially re-stimulated with addition of aAPC as on day 1 of co-culture every 7 days for 5 weeks. Six donors were tested in three independent experiments. Validation of coexpression of CD19, CD64, CD86, CD137L, and IL-15 (eGFP) on aAPC were performed before addition to T-cell cultures as described.⁵ When CD3^{neg}CD56⁺ populations exceeded 10% of the culture, these natural killer cells were depleted using CD56 microbeads (Miltenyi Biotec) and LS columns.⁵ As negative control for CAR and TCR $\gamma\delta$ expression, $\alpha\beta$ T cells from sham-electroporated PBMC (no DNA electrotransferred) were propagated in parallel with OKT3 (CD3-specific monoclonal antibody; Orthoclone)-loaded γ -irradiated aAPC added every 7 days with thrice weekly administration of IL-2, as above.²⁹ CAR^{neg} $\gamma\delta$ T cells were also sorted and expanded on aAPC with IL-2 and IL-21 as undertaken with CAR⁺ $\gamma\delta$ T cells, except that they were not electroporated, and these cells were used for cytotoxicity experiments. 10⁷ PBMC were cultured with a single dose of Zol (1 μ g/ml; Novartis) with thrice weekly additions of IL-2 and IL-21, as above, to expand CAR^{neg} V γ 9V δ 2 T cells.

Flow cytometry. Cultures were phenotyped using antibodies detailed in **Supplementary Table S1**. Appropriate isotype controls were used to validate gating. Staining was performed in FACS buffer (phosphate-buffered saline, 2% fetal bovine serum, 0.1% sodium azide) for 20–30 minutes at

4°C, and two washes with FACS buffer were performed before staining and between stains. Intracellular staining was done following fixation and permeabilization for 20 minutes at 4°C with BD Cytotfix/Cytoperm (BD Biosciences, San Diego, CA). Intracellular staining was performed in Perm/Wash buffer, 10% human AB serum for 30 minutes at 4°C. FITC, PE, PerCP/Cy5.5, and APC antibodies were used at 1:20, 1:40, 1:33, and 1:40 dilutions, respectively. All samples were acquired on FACSCalibur (BD Biosciences) and analyzed with FlowJo software (version 7.6.3; TreeStar, Ashland, OR).

Direct imaging of mRNA molecules by DTEA. At days 0 and 36 of co-culture on aAPC, at least 10⁵ T cells were lysed at a ratio of 5 μ l RLT Buffer (Qiagen, Valencia, CA) per 3 \times 10⁴ cells and frozen at –80°C in replicate vials for one time use. RNA lysates were thawed and immediately analyzed using nCounter Analysis System (NanoString Technologies, Seattle, WA) following a minimum of 12 hours hybridization at 65°C using multiplexed target-specific color-coded reporter and biotinylated capture probes to detect mRNAs of interest. Two CodeSets were generated from RefSeq accession numbers for selected mRNA transcripts and were used to generate the specific reporter and capture probe pairs for the designer TCR expression array (DTEA, **Supplementary Table S2**). Reporter-capture nCounter probe pairs were identified that (i) minimized off-target effects due to cross-hybridization of reporter-capture probe pairs to non-target molecules, (ii) target most, if not all, of the transcript variants for a particular gene, and (iii) efficiently hybridize. Five reference genes that span the dynamic range of RNA expression in lymphocytes (ACTB, OAZ1, POLR1B, POLR2A, and RPL27) were included to normalize transcript levels between different samples and to account for differences in the amount of total RNA present in the samples. A normalization factor for each sample was derived from the formula ($\sum_{total} / \sum_{sample}$) and then applied to each sample that had been background subtracted. Percentage of V δ and V γ were then calculated based on normalized values.

Cytokine production and secretion. T cells harvested at day 35 of co-culture on γ -irradiated aAPC were examined for cytokine secretion by multiplex analysis and expression by intracellular staining. The former was set up with triplicate overnight co-cultures of 10⁵ genetically modified T cells and (i) mock (complete media), (ii) leukocyte activation cocktail (5 ng/ml PMA (Sigma, St Louis, MO), 500 ng/ml ionomycin (Sigma)), (iii) 10⁵ CD19^{neg} EL4 cells, or (iv) 10⁵ CD19⁺ EL4 cells. Supernatants were harvested the following day and like wells were pooled and frozen at –80°C until time of analysis. Samples were then thawed on ice, diluted 1:8 in complete media, and interrogated on Bio-Plex Pro Human Cytokine 27-plex Assay (Bio-Rad, Hercules, CA) according to manufacturer's instructions using Luminex100 (xMap Technologies, Austin, TX). Intracellular cytokine production was established from similar conditions as above, except (i) 5 \times 10⁵ EL4 cells were used, (ii) the incubation period was 6 hours, and (iii) the secretory pathway inhibitor GolgiPlug (BD Biosciences) containing brefeldin A was added at 1:1,000 dilution.

Chromium release assay. *In vitro* cytolytic capability was assessed using standard 4-hour chromium release assay as previously described.⁵

Mouse experiments. *In vivo* antitumor efficacy was assessed in NSG mice (NOD.Cg-Prkdc^{scid} Il2r ^{γ m1Wj}/SzJ; Jackson Laboratories, Bar Harbor, ME). The day after intravenous injection of 10⁵ NALM6-*ffLuc*-eGFP, experimental groups ($n = 5$) received (i) no treatment or (ii) 10⁷ CAR⁺ $\gamma\delta$ T cells. As controls for potential graft-versus-host-disease, three NSG mice received CAR⁺ $\gamma\delta$ T cells without tumor. T cells were administered every 7 days for three doses along with 6 \times 10⁴ IU/injection recombinant human IL-2 at the time of infusion and twice on the day after (**Figure 6a**). Noninvasive bioluminescent imaging to measure tumor burden of NALM6-*ffLuc*-eGFP was performed during the course of the experiments following subcutaneous D-Luciferin (Caliper, Hopkinton, MA) administration on IVIS-100 Imager (Caliper). Bioluminescent imaging was analyzed using Living

Image software (version 2.50, Xenogen; Caliper). Tumor burden in peripheral blood leukocytes, spleens, and bone marrow was evaluated by flow cytometry postmortem.

SUPPLEMENTARY MATERIAL

Figure S1. Distribution of $V\delta$ and $V\gamma$ in $\gamma\delta$ T cells expanded on aminobisphosphonate.

Figure S2. Specific lysis of CD19⁺ tumor cell lines by CAR⁺, CAR⁺⁺, and CAR⁺⁺⁺ $\gamma\delta$ T cells.

Figure S3. *Sleeping Beauty* DNA transposon (designated Δ CD19-F2A-Neo) to coexpress truncated human CD19 and neomycin phosphotransferase for *in vitro* selection.

Table S1. Antibodies used in study.

Table S2. Direct TCR expression assay.

ACKNOWLEDGMENTS

D.C.D. is a Teal Pre-doctoral Scholar (DOD Ovarian Cancer Research Program), American Legion Auxiliary Fellow in Cancer Research (UT-GSBS at Houston), and Andrew Sowell-Wade Huggins Scholar in Cancer Research (UT-GSBS at Houston and Cancer Answers Foundation). The Immune Monitoring Core Lab (IMCL, MD Anderson Cancer Center) performed Luminex analysis. We thank Perry Hackett from University of Minnesota for help with *Sleeping Beauty* system and Carl June from University of Pennsylvania for assistance in generating the K562-derived artificial antigen-presenting cell (clone #4). This work was supported by funding from: Cancer Center Core grant (CA16672); RO1 (CA124782, CA120956, CA141303; CA163587); R33 (CA116127); P01 (CA148600); SPORE (CA136411, CA100632); S10RR026916; AdeeeHeebe; Albert J. Ward Foundation; Ahuja family; Burroughs Wellcome Fund; Cancer Prevention and Research Institute of Texas; Caryn Papantonakis; CLL Global Research Foundation; Department of Defense; Estate of Noelan L. Bibler; Gillson Longenbaugh Foundation; Harry T Mangurian, Jr., Fund for Leukemia Immunotherapy; Fund for Leukemia Immunotherapy; Institute of Personalized Cancer Therapy; Leukemia and Lymphoma Society; Lymphoma Research Foundation; Miller Foundation; Mr and Mrs Rick Calhoun; Mr Herb Simons; Mr and Mrs Joe H Scales; Mr Thomas Scott; National Foundation for Cancer Research; Paula Gavrel Asher Foundation; Pediatric Cancer Research Foundation; Production Assistance for Cellular Therapies; Robert J. Kleberg, Jr. and Helen C. Kleberg Foundation; Team Connor; Thomas Scott; William Lawrence and Blanche Hughes Children's Foundation. This work was performed in Houston, TX, USA. The authors declared no conflict of interest.

REFERENCES

- Singh, H, Manuri, PR, Olivares, S, Dara, N, Dawson, MJ, Huls, H *et al.* (2008). Redirecting specificity of T-cell populations for CD19 using the Sleeping Beauty system. *Cancer Res* **68**: 2961–2971.
- Kowolik, CM, Topp, MS, Gonzalez, S, Pfeiffer, T, Olivares, S, Gonzalez, N *et al.* (2006). CD28 costimulation provided through a CD19-specific chimeric antigen receptor enhances *in vivo* persistence and antitumor efficacy of adoptively transferred T cells. *Cancer Res* **66**: 10995–11004.
- Jena, B, Dotti, G and Cooper, LJ (2010). Redirecting T-cell specificity by introducing a tumor-specific chimeric antigen receptor. *Blood* **116**: 1035–1044.
- Cooper, LJ, Topp, MS, Serrano, LM, Gonzalez, S, Chang, WC, Naranjo, A *et al.* (2003). T-cell clones can be rendered specific for CD19: toward the selective augmentation of the graft-versus-B-lineage leukemia effect. *Blood* **101**: 1637–1644.
- Singh, H, Figliola, MJ, Dawson, MJ, Huls, H, Olivares, S, Switzer, K *et al.* (2011). Reprogramming CD19-specific T cells with IL-21 signaling can improve adoptive immunotherapy of B-lineage malignancies. *Cancer Res* **71**: 3516–3527.
- Brentjens, RJ, Riviere, I, Park, JH, Davila, ML, Wang, X, Stefanski, J *et al.* (2011). Safety and persistence of adoptively transferred autologous CD19-targeted T cells in patients with relapsed or chemotherapy refractory B-cell leukemias. *Blood* **118**: 4817–4828.
- Porter, DL, Levine, BL, Kalos, M, Bagg, A and June, CH (2011). Chimeric antigen receptor-modified T cells in chronic lymphoid leukemia. *N Engl J Med* **365**: 725–733.
- Kalos, M, Levine, BL, Porter, DL, Katz, S, Grupp, SA, Bagg, A *et al.* (2011). T cells with chimeric antigen receptors have potent antitumor effects and can establish memory in patients with advanced leukemia. *Sci Transl Med* **3**: 95ra73.
- Kochenderfer, JN, Wilson, WH, Janik, JE, Dudley, ME, Stetler-Stevenson, M, Feldman, SA *et al.* (2010). Eradication of B-lineage cells and regression of lymphoma in a patient treated with autologous T cells genetically engineered to recognize CD19. *Blood* **116**: 4099–4102.
- Castella, B, Vitale, C, Coscia, M and Massaia, M (2011). $V\gamma9V\delta2$ T cell-based immunotherapy in hematological malignancies: from bench to bedside. *Cell Mol Life Sci* **68**: 2419–2432.
- Brandes, M, Willmann, K, Bioley, G, Lévy, N, Eberl, M, Luo, M *et al.* (2009). Cross-presenting human gammadelta T cells induce robust CD8⁺ alpha beta T cell responses. *Proc Natl Acad Sci USA* **106**: 2307–2312.
- Gomes, AQ, Martins, DS and Silva-Santos, B (2010). Targeting $\gamma\delta$ T lymphocytes for cancer immunotherapy: from novel mechanistic insight to clinical application. *Cancer Res* **70**: 10024–10027.
- Scotet, E, Martinez, LO, Grant, E, Barbaras, R, Jenö, P, Guiraud, M *et al.* (2005). Tumor recognition following $V\gamma$ 9 $V\delta$ 2 T cell receptor interactions with a surface F1-ATPase-related structure and apolipoprotein A-I. *Immunity* **22**: 71–80.
- Hayday, AC (2000). $[\gamma\delta]$ cells: a right time and a right place for a conserved third way of protection. *Annu Rev Immunol* **18**: 975–1026.
- Kondo, M, Sakuta, K, Noguchi, A, Ariyoshi, N, Sato, K, Sato, S *et al.* (2008). Zoledronate facilitates large-scale *ex vivo* expansion of functional gammadelta T cells from cancer patients for use in adoptive immunotherapy. *Cytotherapy* **10**: 842–856.
- Chiplunkar, S, Dhar, S, Wesch, D and Kabelitz, D (2009). gammadelta T cells in cancer immunotherapy: current status and future prospects. *Immunotherapy* **1**: 663–678.
- Lamb, LS Jr, Henslee-Downey, PJ, Parrish, RS, Godder, K, Thompson, J, Lee, C *et al.* (1996). Increased frequency of TCR gamma delta + T cells in disease-free survivors following T cell-depleted, partially mismatched, related donor bone marrow transplantation for leukemia. *J Hematol* **5**: 503–509.
- Lamb, LS Jr, Gee, AP, Hazlett, LJ, Musk, P, Parrish, RS, O'Hanlon, TP *et al.* (1999). Influence of T cell depletion method on circulating gammadelta T cell reconstitution and potential role in the graft-versus-leukemia effect. *Cytotherapy* **1**: 7–19.
- Lamb, LS Jr, Musk, P, Ye, Z, van Rhee, F, Geier, SS, Tong, JJ *et al.* (2001). Human gammadelta(+) T lymphocytes have *in vitro* graft vs leukemia activity in the absence of an allogeneic response. *Bone Marrow Transplant* **27**: 601–606.
- Godder, KT, Henslee-Downey, PJ, Mehta, J, Park, BS, Chiang, KY, Abhyankar, S *et al.* (2007). Long term disease-free survival in acute leukemia patients recovering with increased gammadelta T cells after partially mismatched related donor bone marrow transplantation. *Bone Marrow Transplant* **39**: 751–757.
- Numbenjapon, T, Serrano, LM, Singh, H, Kowolik, CM, Olivares, S, Gonzalez, N *et al.* (2006). Characterization of an artificial antigen-presenting cell to propagate cytolytic CD19-specific T cells. *Leukemia* **20**: 1889–1892.
- Zhang, M, Maiti, S, Bernatchez, C, Huls, H, Rabinovich, B, Champlin, RE *et al.* (2012). A new approach to simultaneously quantify both Tcr α - and β -chain diversity after adoptive immunotherapy. *Clin Cancer Res: Off J Am Soc Cancer Res* **18**(17): 4733–4742.
- Rischer, M, Pscherer, S, Duwe, S, Vormoor, J, Jürgens, H and Rossig, C (2004). Human gammadelta T cells as mediators of chimaeric-receptor redirected anti-tumour immunity. *Br J Haematol* **126**: 583–592.
- Hanrahan, CF, Kimpton, WG, Howard, CJ, Parsons, KR, Brandon, MR, Andrews, AE *et al.* (1997). Cellular requirements for the activation and proliferation of ruminant gammadelta T cells. *J Immunol* **159**: 4287–4294.
- Nagamine, I, Yamaguchi, Y, Ohara, M, Ikeda, T and Okada, M (2009). Induction of gamma delta T cells using zoledronate plus interleukin-2 in patients with metastatic cancer. *Hiroshima J Med Sci* **58**: 37–44.
- García, VE, Jullien, D, Song, M, Uyemura, K, Shuai, K, Morita, CT *et al.* (1998). IL-15 enhances the response of human gamma delta T cells to nonpeptide [correction of nonpeptide] microbial antigens. *J Immunol* **160**: 4322–4329.
- Do, JS and Min, B (2009). IL-15 produced and trans-presented by DCs underlies homeostatic competition between CD8 and $[\gamma\delta]$ T cells *in vivo*. *Blood* **113**: 6361–6371.
- Theirez, A, Harly, C, Morice, A, Salot, S, Bonneville, M and Scotet, E (2009). IL-21-mediated potentiation of antitumor cytolytic and proinflammatory responses of human V gamma 9V delta 2 T cells for adoptive immunotherapy. *J Immunol* **182**: 3423–3431.
- O'Connor, CM, Sheppard, S, Hartline, CA, Huls, H, Johnson, M, Palla, SL *et al.* (2012). Adoptive T-cell therapy improves treatment of canine non-Hodgkin lymphoma post chemotherapy. *Sci Rep* **2**: 249.
- Kelly-Rogers, J, Madrigal-Estebas, L, O'Connor, T and Doherty, DG (2006). Activation-induced expression of CD56 by T cells is associated with a reprogramming of cytolytic activity and cytokine secretion profile *in vitro*. *Hum Immunol* **67**: 863–873.
- Smetak, M, Kimmel, B, Birkmann, J, Schaefer-Eckart, K, Einsele, H, Wilhelm, M *et al.* (2008). Clinical-scale single-step CD4(+) and CD8(+) cell depletion for donor innate lymphocyte infusion (DILI). *Bone Marrow Transplant* **41**: 643–650.
- Klebanoff, CA, Gattinoni, L and Restifo, NP (2006). CD8+ T-cell memory in tumor immunology and immunotherapy. *Immunol Rev* **211**: 214–224.
- Di Mitri, D, Azevedo, RI, Henson, SM, Libri, V, Riddell, NE, Macaulay, R *et al.* (2011). Reversible senescence in human CD4+CD45RA+CD27- memory T cells. *J Immunol* **187**: 2093–2100.
- Kulkarni, MM (2011). Digital multiplexed gene expression analysis using the NanoString nCounter system. *Curr Protoc Mol Biol* **Chapter 25**: Unit25B.10.
- Kang, N, Zhou, J, Zhang, T, Wang, L, Lu, F, Cui, Y *et al.* (2009). Adoptive immunotherapy of lung cancer with immobilized anti-TCRgammadelta antibody-expanded human gammadelta T-cells in peripheral blood. *Cancer Biol Ther* **8**: 1540–1549.
- Dokouhaki, P, Han, M, Joe, B, Li, M, Johnston, MR, Tsao, MS *et al.* (2010). Adoptive immunotherapy of cancer using *ex vivo* expanded human gammadelta T cells: A new approach. *Cancer Lett* **297**: 126–136.
- Lopez, RD, Xu, S, Guo, B, Negrin, RS and Waller, EK (2000). CD2-mediated IL-12-dependent signals render human gamma delta T cells resistant to mitogen-induced apoptosis, permitting the large-scale *ex vivo* expansion of functionally distinct lymphocytes: implications for the development of adoptive immunotherapy strategies. *Blood* **96**: 3827–3837.
- Brandes, M, Willmann, K and Moser, B (2005). Professional antigen-presentation function by human gammadelta T Cells. *Science* **309**: 264–268.

39. Newton, DJ, Andrew, EM, Dalton, JE, Mears, R and Carding, SR (2006). Identification of novel gammadelta T-cell subsets following bacterial infection in the absence of Vgamma1+ T cells: homeostatic control of gammadelta T-cell responses to pathogen infection by Vgamma1+ T cells. *Infect Immun* **74**: 1097–1105.
40. Olofsson, K, Hellström, S and Hammarström, ML (1998). The surface epithelium of recurrent infected palatine tonsils is rich in gammadelta T cells. *Clin Exp Immunol* **111**: 36–47.
41. Knight, A, Madrigal, AJ, Grace, S, Sivakumaran, J, Kottaridis, P, Mackinnon, S *et al.* (2010). The role of V δ 2-negative $\gamma\delta$ T cells during cytomegalovirus reactivation in recipients of allogeneic stem cell transplantation. *Blood* **116**: 2164–2172.
42. Stresing, V, Daubiné, F, Benzaid, I, Mönkkönen, H and Clézardin, P (2007). Bisphosphonates in cancer therapy. *Cancer Lett* **257**: 16–35.
43. Angelini, DF, Borsellino, G, Poupot, M, Diamantini, A, Poupot, R, Bernardi, G *et al.* (2004). FcgammaRIII discriminates between 2 subsets of Vgamma9Vdelta2 effector cells with different responses and activation pathways. *Blood* **104**: 1801–1807.
44. Haas, JD, Nistala, K, Petermann, F, Saran, N, Chennupati, V, Schmitz, S *et al.* (2011). Expression of miRNAs miR-133b and miR-206 in the *Il17a/f* locus is co-regulated with IL-17 production in $\alpha\beta$ and $\gamma\delta$ T cells. *PLoS ONE* **6**: e20171.
45. Kryczek, I, Wei, S, Zou, L, Altuwaijri, S, Szeliga, W, Kolls, J *et al.* (2007). Cutting edge: Th17 and regulatory T cell dynamics and the regulation by IL-2 in the tumor microenvironment. *J Immunol* **178**: 6730–6733.
46. Lai, D, Wang, F, Chen, Y, Wang, C, Liu, S, Lu, B *et al.* (2012). Human ovarian cancer stem-like cells can be efficiently killed by $\gamma\delta$ T lymphocytes. *Cancer Immunol Immunother* **61**: 979–989.
47. Middleton, GW, Annels, NE and Pandha, HS (2012). Are we ready to start studies of Th17 cell manipulation as a therapy for cancer? *Cancer Immunol Immunother* **61**: 1–7.
48. Cua, DJ and Tato, CM (2010). Innate IL-17-producing cells: the sentinels of the immune system. *Nat Rev Immunol* **10**: 479–489.
49. Haas, JD, González, FH, Schmitz, S, Chennupati, V, Föhse, L, Kremmer, E *et al.* (2009). CCR6 and NK1.1 distinguish between IL-17A and IFN-gamma-producing gammadelta effector T cells. *Eur J Immunol* **39**: 3488–3497.
50. Paulos, CM, Carpenito, C, Plesa, G, Suhoski, MM, Varela-Rohena, A, Golovina, TN *et al.* (2010). The inducible costimulator (ICOS) is critical for the development of human T(H)17 cells. *Sci Transl Med* **2**: 55ra78.
51. Manuri, PV, Wilson, MH, Maiti, SN, Mi, T, Singh, H, Olivares, S *et al.* (2010). piggyBac transposon/transposase system to generate CD19-specific T cells for the treatment of B-lineage malignancies. *Hum Gene Ther* **21**: 427–437.